IOPscience iopscience.iop.org

Home Search Collections Journals About Contact us My IOPscience

Trapped charge dynamics in a sol–gel based TiO_2 high- k gate dielectric silicon metal–oxide–semiconductor field effect transistor

This article has been downloaded from IOPscience. Please scroll down to see the full text article.

2009 J. Phys.: Condens. Matter 21 215902

(http://iopscience.iop.org/0953-8984/21/21/215902)

View the table of contents for this issue, or go to the journal homepage for more

Download details:
IP Address: 129.252.86.83
The article was downloaded on 29/05/2010 at 19:54

Please note that terms and conditions apply.

J. Phys.: Condens. Matter **21** (2009) 215902 (6pp) doi:10.1088/0953-8984/21/21/215902

Trapped charge dynamics in a sol–gel based TiO_2 high-*k* gate dielectric silicon metal–oxide–semiconductor field effect transistor

M Ziaur Rahman Khan[1], D G Hasko[1], M S M Saifullah[2] and M E Welland[1]

[1] Nanoscience Centre, University of Cambridge, J J Thomson Avenue, Cambridge CB3 0FF, UK
[2] Patterning and Fabrication Capability Group, Institute of Materials Research and Engineering, A*STAR (Agency for Science Technology and Research), 3 Research Link, Singapore 117602, Republic of Singapore

Received 19 August 2008, in final form 7 April 2009
Published 29 April 2009
Online at stacks.iop.org/JPhysCM/21/215902

Abstract

We have studied the response of a sol–gel based TiO_2, high *k* dielectric field effect transistor structure to microwave radiation. Under fixed bias conditions the transistor shows frequency dependent current fluctuations when exposed to continuous wave microwave radiation. Some of these fluctuations take the form of high *Q* resonances. The time dependent characteristics of these responses were studied by modulating the microwaves with a pulse signal. The measurements show that there is a shift in the centre frequency of these high *Q* resonances when the pulse time is varied. The measured lifetime of these resonances is high enough to be useful for non-classical information processing.

(Some figures in this article are in colour only in the electronic version)

1. Introduction

High-*k* dielectric materials are currently being investigated intensively to enable the further downscaling of silicon MOSFETs following Moore's law [1] beyond the limits imposed the breakdown of ultra-thin silicon dioxide gate dielectric layers [2–5]. Titanium oxide (TiO_2) has a high relative permittivity between 4 and 86 and good thermal stability on silicon, would be an attractive high-*k* dielectric material [6–9]. But TiO_2 has a rather small conduction band offset with silicon, which leads to a high gate leakage current at room temperature [3]. The gate leakage current is strongly dependent on the electric field, the temperature and on the nature of the charge traps within the dielectric material [2, 10]. These charge traps can originate through a non-stoichiometry of the dielectric material (particularly oxygen deficiencies in the case of TiO_2) or through the incorporation of impurities (such as organic residues from a sol–gel process that are not completely consumed by the annealing process). The properties of these traps are usually investigated by measuring the DC gate leakage characteristics as a function of electric field and temperature or by measuring the response to a voltage step, so that some time dependent information can be obtained [11–16]. In both cases, the experiment usually requires a non-standard device to give a measurable signal and it is the collective properties of a large number of traps that is determined by such a measurement.

In previous work, a TiO_2 sol–gel based high-*k* gate dielectric silicon MOSFET was fabricated and the characteristics studied over a range of temperatures [17]. At room temperature, rather poor transistor operation was demonstrated due to the high gate leakage current that results from the small conduction band offset and from impurities in the gate dielectric layer. However at reduced temperature, the transistor characteristics were greatly improved due to the suppression of the thermally activated tunnelling that determines the temperature dependence of the leakage current. Good transistor operation was obtained at a temperature of 4 K in a sub-micron MOSFET device. Furthermore, microwave spectroscopy indicated a highly non-linear response that was

 © 2009 IOP Publishing Ltd Printed in the UK

absent at room temperature, but increased in amplitude and visibility as the temperature was reduced. The measured microwave characteristic was different for each device and was modified upon thermal cycling, but was stable and repeatable as long as changes to the gate and source–drain voltages or to the temperature were kept small. Microwave resonances have also been seen in similar devices made using ZrO_2 but were absent in devices made using HfO_2 or without the sol–gel derived high-*k* dielectric. TiO_2 gave the clearest and most stable resonances and so were chosen for further investigation.

It was speculated that the origin of these features was the modification, by the microwave radiation, of the charge trapped in the gate dielectric. The very large number of separately identifiable features in the microwave spectrum suggested that the contributions due to individual traps may be isolated using frequency addressing. If so, then this would offer a method for exploring the properties of individual traps, something that is not possible with conventional approaches. In this paper, we extend the measurement of the microwave characteristics to high resolution microwave spectroscopy, using both continuous wave (CW) and pulsed excitation. Long lived excitations are identified using CW measurements and their time dependence investigated using pulsed measurements.

In practice, the leakage current characteristics of these devices limits useful operation to low temperatures only. But, as the threshold voltage shifts significantly with temperature, the design of conventional circuits using these devices is extremely difficult, so that this structure is best suited for single transistor operation. Since low temperature transistor operation is essential for the read-out device in a solid state quantum computer, the device described in this work may be suitable for this application. The possibility of using this structure as a read-out device, with the charge traps acting as qubits, is discussed.

2. Experimental setup

The fabrication of TiO_2 sol–gel based high-*k* gate dielectric silicon MOSFETs has been described previously [17]. The transistor is designed with nominal channel dimensions of 500 nm in width and 1000 nm in length, made using an SOI wafer with a weakly p-type ($N_A \sim 10^{15}$ cm^{-3}) 50 nm thick silicon layer isolated by a 200 nm thick buried oxide layer from the substrate. The high-*k* dielectric layer was deposited as a TiO_2 sol–gel by spinning and the gate area was crosslinked by e-beam exposure with a dose of 350 C m^{-2}, at a beam energy of 50 kV. After removal of the unexposed material, the remaining TiO_2 was annealed in an air ambient at a temperature of 450 °C for 1 h to remove organic residues, giving a final gate dielectric thickness of 40 nm. Aluminium metallization was used for the gate metal, as well as for the source and drain contact pads.

Individual transistors were bonded into 20 pin leadless header packages for electrical testing in a modified burn-in socket that could be directly immersed into liquid cryogens. DC electrical measurements were made using Keithley 236 SMUs, controlled by a LabView program, through lines that were low pass filtered by Minicircuits BLP1.9 coaxial units (to minimize the effects of external electromagnetic noise). The best signal-to-noise ratios for microwave spectroscopy were obtained with DC biasing close to the threshold condition for the transistor, however the biasing conditions had only a very small effect on the shape of the response seen. The nature of the burn-in socket, the leadless header package and the low pass filter limited the bandwidth for signals passing between the device under test and the room temperature voltage sources and current measurement equipment to a practical frequency of <2 MHz.

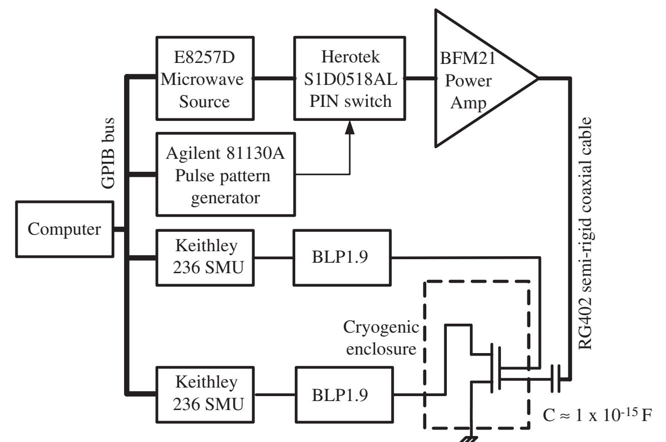

Figure 1. Schematic diagram of the measurement circuit. The microwave signal is carried by an RG402 semi-rigid waveguide to within ∼0.5 mm of the device-under-test, where it is coupled capacitively to the gate and/or source/drain electrodes. The dashed line marks the cryogenic enclosure (this forms a Faraday cage of ∼1 m in length) that is directly immersed into the liquid cryogens.

The schematic diagram of the circuit arrangement is shown in figure 1. Continuous microwaves (CW), in the frequency range 0.25 to ∼4 GHz, were provided by an Agilent E8257D PSG Analog Signal Generator and coupled to the device under test by an open ended RG402 semi-rigid coaxial waveguide. By controlling the spacing between the end of the waveguide and the base of the header package containing the device under test, reflections from the end of the waveguide may be avoided over a wide frequency range, at the expense of very weak coupling of the microwave power to the device under test. By not having a direct connection to the device under test, the heat load due to thermal conduction along the waveguide is eliminated.

Pulsed microwave signals were obtained by passing the CW signal through a Herotek S1D0518AL SPST PIN switch controlled by an Agilent 81130A pulse pattern generator. The microwave signal was further amplified by an AH1-1 MMIC amplifier (WJ Communications Inc.) situated about 1 m away from the device under test.

3. Results and discussion

The DC characterization of these devices has been reported previously [17], where transistor operation was observed at room temperature, 77 and 4 K. In this work we concentrate

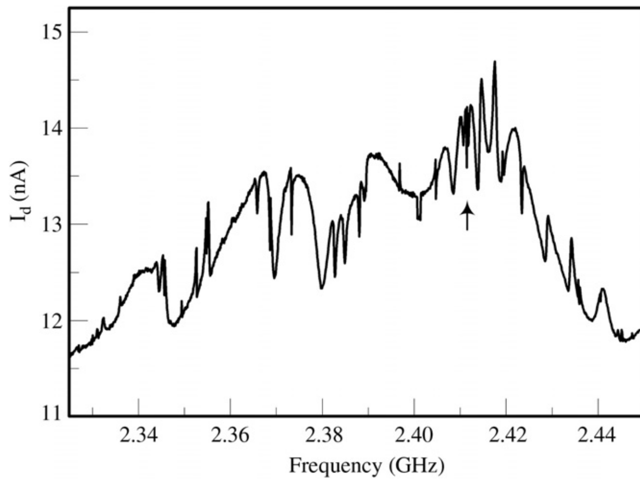

Figure 2. Wideband microwave spectroscopy for a device with source–drain bias of 1.0 V and gate voltage 1.1 V. The arrow indicates the position of a high Q resonance used for the subsequent pulse time dependence measurement.

on the device behaviour measured at a temperature of 4 K, using fixed gate and source–drain bias voltages close to the threshold condition. The drain current response to wideband microwave spectroscopy, using a CW signal power of about +12 dBm applied to the room temperature end of the coupling waveguide, is shown in figure 2. This spectrum shows two types of feature; those of large amplitude (~25% of nominal current) that change relatively slowly with frequency and smaller amplitude features ($\lesssim$5% of nominal current) that occur over significantly smaller frequency ranges. These latter features show as spikes in this figure, but are resolved into resonant peaks with well defined linewidth, when measured at high resolution. In the accessible frequency range, there are several hundred such resonances. We concentrate on the latter features for the remainder of the paper.

In order to investigate the time dependent behaviour of these resonances, we amplitude modulate the microwave signal with equal ON and OFF times, together being the pulse time. This modulation is seen to have a significant effect on the behaviour, an example for a typical resonance is shown in figure 3(a). This colour map shows the change in time averaged device current as a function of microwave frequency and modulation pulse time; each measurement point takes ~200 ms corresponds to a very large number of individual modulation pulses. The centre frequency of this resonance is indicated by the diagonal green feature starting at 2.4104 GHz for the shortest pulse time and ending at 2.4108 GHz for a pulse time of 10 μs. The CW behaviour of this resonance is shown in the inset, which indicates that the resonance is a local decrease in the device current as the frequency is swept through the feature. This behaviour results in the resonant feature being green in the colour plot, a lower current compared to the red/yellow currents seen further away. The square modulation of the microwaves also gives rise to the sideband features seen symmetrically placed above and below the central feature; the frequency separation between these sideband features and the central resonance is inversely dependent on the pulse time

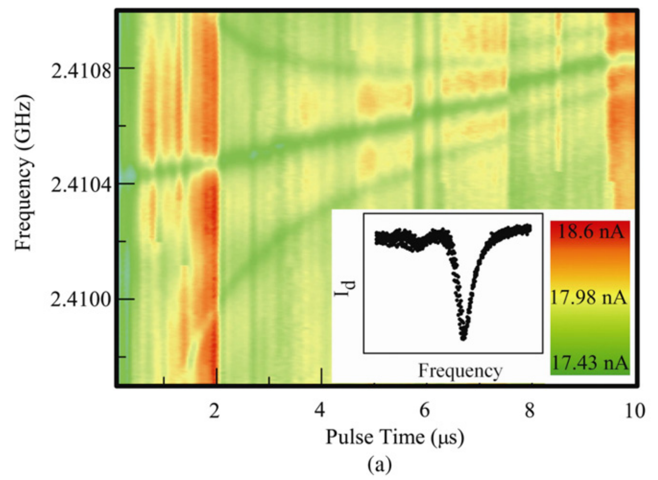

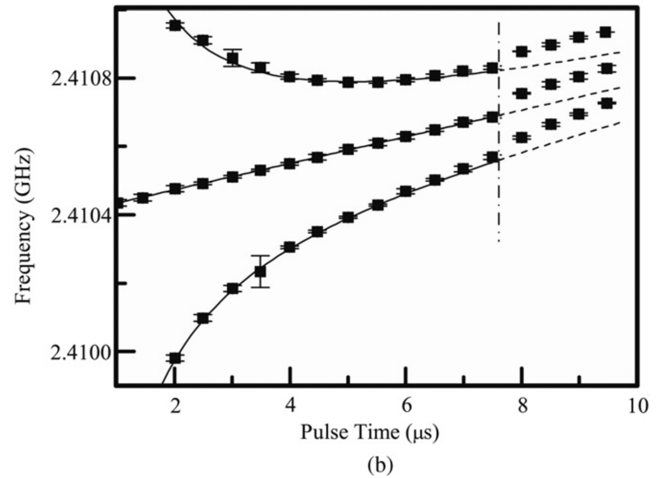

Figure 3. (a) Colour map of the time averaged device current versus pulse time over a limited frequency range about a resonant feature results in a local reduction in current. Inset: CW response of this resonant feature showing a Q factor of ~75 000. (b) The error bars indicating the centre and sideband frequencies determined from (a) and the continuous line represents the sideband calculated using the centre frequency line as a reference. The vertical dot–dashed line indicates where a RTS event occurred.

(figure 3(b)). For the very shortest pulse times the sidebands are moved outside of the range of frequencies in the colour plot. The vertical dashed line represents the point where the random telegraph signal (RTS) occurred and there is an upward shift in the location of the centre peak and sidebands.

At a pulse time of ~7.5 μs a random telegraph event occurred, which caused an overall step change in the measured current; this step change coincided with a stepwise increase in the resonant and sideband frequencies of ~50 kHz. These kind of stepwise current changes are usually attributed to the emptying or filling of individual traps [18], suggesting that the charge stored in a nearby trap has a significant effect on the centre frequency of this resonant feature. Other random telegraph events are visible in the colour plot, although most show little or no influence on the centre frequency of the resonance. This is understandable if the traps causing such events are situated at a long distance from that causing the resonant feature; such a large separation is more likely than close proximity due to the geometry of the device.

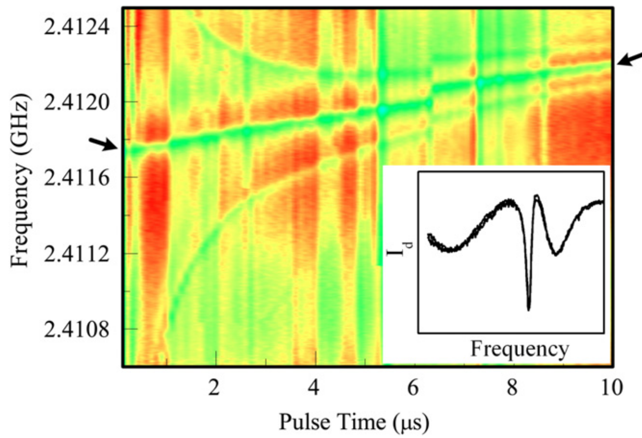

Figure 4. Colour map of the time averaged device current versus pulse time over a limited frequency range about another resonant feature. Similar behaviour to that seen in figure 3 is seen, including an increase in centre and sideband frequencies with increasing pulse time of similar magnitude. Arrows indicate the centre frequency at the shortest and the longest pulse times. Inset: CW response of this feature showing a Q factor of ~61 000.

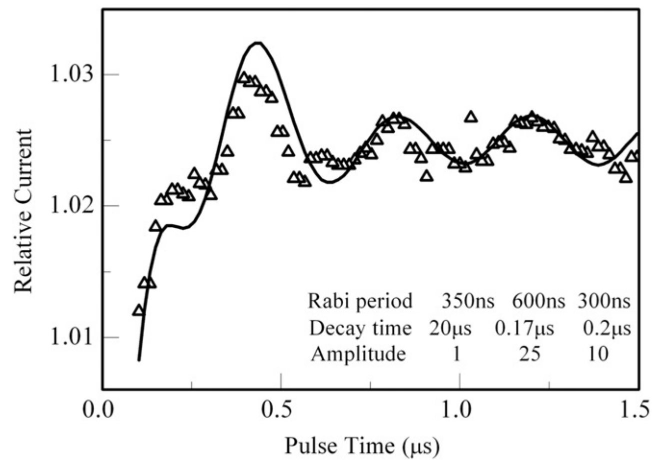

Figure 5. Relative centre peak amplitude for the resonance shown in figure 3. The continuous line shows the model response due to three components. The first is due to the resonance shown in the inset of figure 3, where a lifetime of about 20 μs has been used, slightly shorter than the value indicated by the CW behaviour due to the increased MW power used in the pulsed measurement. The other two features are due to the sideband excitation of nearby resonant peaks as figure 3.

The pulse time dependence of another feature located at a frequency of ~2.4117 GHz is shown in figure 4. Very similar behaviour compared to that in figure 3 is observed, including the positive slope of the pulse time dependence of the centre frequency (~40 kHz μs^{-1}) suggesting that this behaviour may be universal.

The Q value and centre frequency (f_0) of the resonance suggests that coherent behaviour is possible over a time period approximately equal to the ratio (Q/f_0). The amplitude measured along the track of the centre frequency for the data shown in figure 3 is shown in figure 5. The shift in centre frequency due to random telegraph events does not allow us to extend this graph to the full extent of the data shown in figure 3, although arbitrarily offsetting the track suggests that the observed behaviour is maintained over the full pulse time range. There is a strong pulse time dependence of the amplitude, which extends throughout the range of measurements, although the largest changes occur at the shortest pulse times.

Coherent behaviour would be indicated by an oscillation of the amplitude with a decay time given by the ratio (Q/f_0). In addition to this decaying sine wave, we have a contribution to the amplitude change from the sidebands, which can interact with nearby peaks, particularly for the shortest pulse times. The CW data shown in the inset in figure 3 shows that there are no additional resonant peaks within the measured frequency range, which corresponds to pulse times down to ~1 μs. The continuous line in figure 5 shows a fit to the measured data using the period and taking the decay time from the ratio (Q/f_0), together with two other terms corresponding to nearby resonances. For the data in figures 3 and 5, these additional contributions are significant only for pulse times of less than ~1 μs, which is what is observed in the data.

We now discuss the origin of the resonant behaviour, in particular the mechanisms for the change in current with excitation frequency, for the lifetime for this excitation and for the pulse time dependence of the modulated excitation. It is well known that high-k dielectric materials contain significant numbers of traps [3], indeed the sol–gel based material used here probably contains significantly higher numbers of traps than is normally encountered. Charge transport through the high-k dielectric layer takes place through hopping between trapping sites in pathways oriented perpendicular to the silicon surface due to the gate electric field [2]. In this type of transport, the current flow behaviour is always dominated by the hardest hops, so that charge may be isolated in a section of the pathway by two particularly hard hops, as shown schematically in figure 6(a). In the isolated section, we will assume that a single electron can take one of two spatially separated locations. This assumption is justified if each location is formed by an atomic sized defect (such as an oxygen deficiency or carbon atom) as Coulomb charging will prevent more than one extra electron being accommodated on the site and if the sites are separated by a sufficiently large (and wide) barrier to ensure charge localization.

In principle, each defect could form a pathway with every other nearby defect, however, in practice, we need only be concerned with the pathways formed by the much smaller subset of defect locations where the barrier height/width and energy level separation are small. The electric field and temperature dependence of a large number of such pathways is described by a trap assisted tunnelling mechanism [19]. In the case of the random telegraph events and of the microwave resonances, the change in the channel current is due to a relocation of the charge in one of these isolated regions. This changes the electron number in the channel by a discrete amount, leading to a corresponding change in the channel current.

Trap energy levels will be distributed over a wide energy range due to the disorder in the system, but in some of the

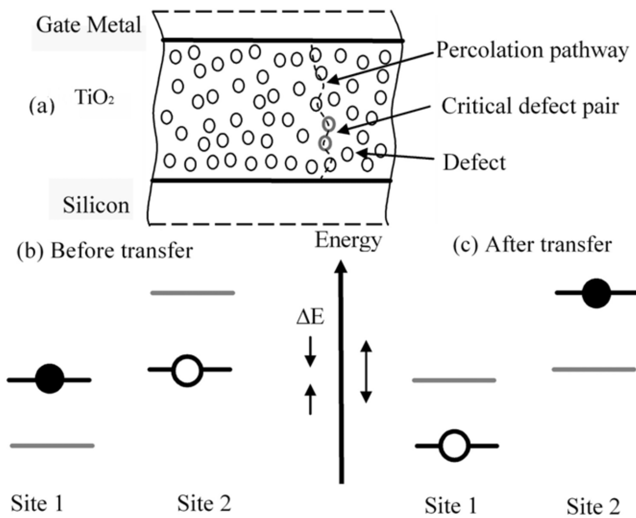

Figure 6. (a) Schematic cross-sectional diagram of the gate dielectric stack showing the location of defects and possible percolation pathways. For any given pathway, the transport may be controlled by charged trapped in a critical pair of defects. (b) Energy level diagram before electron transfer between sites in the critical pair showing the occupied level on the first site (●) and the available unoccupied level on the second site (○). The full lines and the dashed lines represent the energy levels taking account of the on site charge interaction. (c) Energy level diagram after electron transfer.

regions of interest the energy difference between the pair of isolated locations will be small enough to correspond to photon energies in the microwave range. Resonant excitation by an external microwave field will cause spacial Rabi oscillations between the two locations with a corresponding effect on the channel current [20]. Under CW excitation, the Rabi oscillations are not resolved in time with measurement arrangement, but if one of the two locations is preferred for occupation, then these Rabi oscillations have the effect of spreading the occupation from the preferred site to the non-preferred site. This relocation of the trapped electron causes a change in the channel current that is measured as the resonance feature in the microwave spectroscopy.

Boltzmann statistics would suggest that the occupation of two energy levels separated by an energy difference corresponding to a photon frequency of a few GHz is very nearly equal, even at a temperature of 4 K. However, if the barrier between the two locations is sufficiently large that the electron can be considered as localized at one or other location as assumed, then the thermally activated transfer between these locations is rather slow. Moreover, the energy level at each location is not fixed, but is dependent on electrostatic interactions with other nearby charges in the manner of a polaron. One possible consequence is that a preferred location can arise due to the on site contribution to energy level.

Consider the energy level diagram shown in figure 6(b); each location has two energy levels, one corresponding to the occupied state (higher level) and the other corresponding to the unoccupied state (lower level). The energy difference between the occupied and unoccupied levels is due to the electrostatic interaction with other nearby charges and can be expected to be much larger than the microwave photon energy due to the size of the trap and the separation from other charges. On transfer of the electron from the preferred location to the non-preferred location, the energy level separation between the newly occupied and unoccupied levels is considerably increased, see figure 6(c). This changes the thermally activated transfer rate so that the reverse transfer rate is much higher than the forward rate; this anisotropy in the transfer rates essentially localizes the electron on the preferred location in the absence of resonant microwave excitation.

When a resonant microwave excitation is applied to this system spacial Rabi oscillations are set up between the two locations at a frequency that is dependent on the coupled power. At low power, the Rabi frequency is small compared to the thermally activated reverse transfer rate and the occupation of the non-preferred location is unaffected. At higher powers, the Rabi frequency becomes larger than the thermally activated reverse transfer rate so that the occupation of the non-preferred location increases towards a maximum value of 50%.

When the resonant microwave excitation is modulated, the system is in phase with the microwaves only during the ON part of the modulation. During the OFF part of the modulation, the phase of the system lags the microwave source due to the energy losses. The maximum amplitude of a driven simply harmonic system occurs at a higher frequency than the undriven natural frequency; the difference in frequency is related to the losses in the system. In a high Q resonance the losses are small, so that this frequency difference is also small and may be accounted for by adding a linear time dependent phase term to the microwave oscillation to describe the system oscillation. The result of this time dependent phase term is that when the next ON part of the modulation occurs, there is a phase difference between the system oscillation and the microwave signal that is dependent on the OFF time. As the pulse time is increased, this phase difference increases linearly and an amplitude oscillation is completed every time the phase difference exceeds 2π.

4. Conclusions

The behaviour of a TiO_2 sol–gel based high-k gate dielectric silicon MOSFET has been investigated under CW and pulsed microwave irradiation. Coherent behaviour, related to the movement of charge trapped in defects within the dielectric layer, has been observed. This behaviour offers a method for the investigation of the properties of individual traps. The lifetime and detectability of these microwave excitations are promising for use as qubits. A single transistor contains a large number of potential qubits, which can be separately addressed in the frequency domain.

Acknowledgments

M Z R Khan would like to thank the Commonwealth Scholarship Commission for providing financial assistance; D G Hasko and M E Welland acknowledge financial support from the EPSRC funded IRC in Nanotechnology. Special thanks to Jongjin Lee for his help with the LabView program.

References

[1] Moore G 1975 *IEDM Technol. Dig.* **21** 11
[2] Locquet J P, Marchiori C, Sousa M and Fompeyrine J 2006 *J. Appl. Phys.* **100** 051610
[3] Robertson J 2004 *Eur. Phys. J. Appl. Phys.* **28** 265
[4] Wilk G D, Wallace R M and Anthony J M 2001 *J. Appl. Phys.* **89** 5243
[5] Witte H D *et al* 2003 *J. Electrochem. Soc.* **150** F169
[6] Naitou Y *et al* 2008 *Appl. Phys. Lett.* **92** 012112
[7] Campbell S A, Kim H-S, Gilmer D C, He B, Ma T and Gladfelter W L 1999 *IBM J. Res. Dev.* **43** 383
[8] Kadoshima M *et al* 2003 *Thin Solid Films* **424** 224
[9] van Dover R B 1999 *Appl. Phys. Lett.* **74** 3041
[10] Houssa M, Naili M, Heyns M M and Stesmans A 2001 *J. Appl. Phys.* **89** 792
[11] Mahapatra R *et al* 2007 *J. Vac. Sci. Technol.* B **25** 217
[12] Dittrich T *et al* 2000 *Mater. Sci. Eng.* B **69/70** 489
[13] Bera M K and Maiti C K 2007 *Semicond. Sci. Technol.* **22** 774
[14] Gusev E (ed) 2006 *Defects in High-k Gate Dielectric Stacks* (*NATO Science Series II* vol 220) (Dordrecht: Springer)
[15] Bera M K and Maiti C K 2006 *Mater. Sci. Semicond. Process.* **9** 909
[16] Gusev E P *et al* 2001 *Microelectron. Eng.* **59** 341
[17] Khan M Z R, Hasko D G, Saifullah M S M and Welland M E 2008 *J. Vac. Sci. Technol.* B **26** 1887
[18] Schulz M and Karmann A 1991 *Phys. Scr.* T **35** 273
[19] Sze S M 1981 *Physics of Semiconductor Devices* (New York: Wiley)
[20] Foot C J 2005 *Atomic Physics* (New York: Oxford University Press)